
Correlating EGFR Expression with Receptor-Binding Properties and Internalization of ^{64}Cu -DOTA-Cetuximab in 5 Cervical Cancer Cell Lines

Martin Eiblmaier¹, Laura A. Meyer¹, Mark A. Watson², Paula M. Fracasso³, Linda J. Pike⁴, and Carolyn J. Anderson^{1,5}

¹Mallinckrodt Institute of Radiology, Washington University School of Medicine, St. Louis, Missouri; ²Department of Pathology and Immunology, Washington University School of Medicine, St. Louis, Missouri; ³Department of Medicine, Washington University School of Medicine, St. Louis, Missouri; ⁴Department of Biochemistry, Washington University School of Medicine, St. Louis, Missouri; and ⁵Department of Chemistry, Washington University School of Medicine, St. Louis, Missouri

The anti-epidermal growth factor receptor (anti-EGFR) antibody cetuximab is clinically approved for the treatment of EGFR-expressing metastatic colorectal cancer and advanced head and neck cancer. Overexpression of EGFR has also been found in more than 70% of carcinomas of the cervix. The overall goal of this study was to determine whether ^{64}Cu -1,4,7,10-tetraazacyclododecane-*N,N',N'',N'''*-tetraacetic acid (DOTA)-cetuximab has potential as an agent for measuring EGFR concentration by PET imaging in cervical cancer tumors. **Methods:** Cetuximab was conjugated to the bifunctional chelator DOTA and labeled with ^{64}Cu . EGFR messenger RNA (mRNA) expression was correlated with EGFR densities on the cell surface of 5 different cervical cancer cell lines and with receptor function, measured by internalization of ^{64}Cu -DOTA-cetuximab. Imaging in tumor-bearing mice with small-animal PET was performed using the highest-expressing cervical cancer cell line. **Results:** The affinity of ^{64}Cu -DOTA-cetuximab binding for the EGFR was similar in 4 EGFR-positive lines, varying from 0.1 to 0.7 nM. The mRNA expression corresponded well with EGFR densities and levels of internalization, with responses decreasing in the order of CaSki > ME-180 > DoTc2 4510 > HeLa > C-33A. Biodistribution and small-animal PET studies with ^{64}Cu -DOTA-cetuximab in CaSki tumor-bearing nude mice showed relatively high tumor uptake at 24 h after injection (13.2 ± 1.2 percentage of injected activity per gram), although there was also significant retention of activity in the blood and liver accumulation. **Conclusion:** ^{64}Cu -DOTA-cetuximab was successfully used to detect and quantify EGFR expression in cervical cancer tumors, and small-animal PET/CT of EGFR-expressing CaSki tumors suggests potential for PET/CT of EGFR-positive tumors.

Key Words: ^{64}Cu ; cervical cancer; cetuximab

J Nucl Med 2008; 49:1472–1479

DOI: 10.2967/jnumed.108.052316

Received Feb. 29, 2008; revision accepted May 12, 2008.
For correspondence or reprints contact: Carolyn J. Anderson, Mallinckrodt Institute of Radiology, 510 S. Kingshighway Blvd., Campus Box 8225, St. Louis, MO 63110.
E-mail: andersoncj@wustl.edu
COPYRIGHT © 2008 by the Society of Nuclear Medicine, Inc.

Cervical cancer is the most common gynecologic cancer worldwide. In the United States in 2004, more than 10,500 women were diagnosed and 3,900 died (1). Although the majority of women present with early-stage disease and are treated successfully with surgery or radiation, 25% of women present with advanced disease. Current treatment for locally advanced cervical cancer consists of cisplatin-based chemotherapy and concurrent radiation. Overall survival rates with this treatment are low, approximately 52% at 5 y (2).

The epidermal growth factor receptor (EGFR) is a member of the pro-survival ErbB family of receptors. Increased expression of EGFR is the hallmark of many human tumors such as cervical cancer, breast cancer, squamous cell carcinoma of the head and neck, and prostate cancer (3,4).

The role of EGFR in the tumorigenesis of cervical cancer has been debated over the last decade. In one study, overexpression of EGFR was found in 72.5% of patients with invasive cervical cancer and in 25% of patients with cervical intraepithelial neoplasia (5). Larger tumors had significantly higher receptor levels, suggesting that EGFR may play a role in malignant transformation. However, 2 subsequent reports suggested that EGFR is not related to the prognosis of cervical cancer (6) or that the EGFR may be downregulated in most cases of cervical cancer (7). In the latter study, only 10% of tumors showed overexpression of EGFR, compared with normal cervical epithelium. More recent studies have established the role of EGFR overexpression as a predictor of poor prognosis in cervical cancer (8) and have associated EGFR with a poorer prognosis of disease-free and overall survival (9). Coexpression of EGFR and COX-2 was also found to be a potent molecular risk factor in carcinomas of the cervix (10).

The fraction of cervical cancers overexpressing EGFR is presently 54%–74% (3). Thus, pharmaceuticals targeting

EGFR could provide options for diagnostic tools and treatment, at least in certain subtypes of cervical carcinomas. Cetuximab was the first monoclonal antibody targeted against the ligand-binding site of EGFR to be approved by the Food and Drug Administration for the treatment of patients with EGFR-expressing, metastatic colorectal carcinoma. We, therefore, sought to investigate the use of cetuximab for targeting the EGFR in cervical cancer.

We conjugated cetuximab with the bifunctional chelator 1,4,7,10-tetraazacyclododecane-*N,N',N'',N'''*-tetraacetic acid (DOTA) and radiolabeled DOTA-cetuximab with ^{64}Cu . In this study, we compare EGFR messenger RNA (mRNA) levels with cell-surface EGFR expression and receptor internalization, measured using ^{64}Cu -DOTA-cetuximab, in several cervical cancer cell lines. We report that EGFR gene expression correlated with cell-surface EGFR expression and with the extent of uptake of ^{64}Cu -DOTA-cetuximab into tumor cells. We further show that ^{64}Cu -DOTA-cetuximab is an effective PET agent in tumors expressing high levels of EGFR. These data suggest that ^{64}Cu -DOTA-cetuximab may be useful for quantifying EGFR expression in tumors by PET.

MATERIALS AND METHODS

Materials

DOTA-mono-*N*-hydroxysuccinimide ester (DOTA-mono-NHS ester) was purchased from Macrocylics. Centricon 100 concentrators were purchased from Amicon Inc. All other chemicals were purchased from Aldrich Chemical Co. All buffers were prepared using distilled deionized water (resistivity, $\sim 18\ \text{M}\Omega$) (Milli-Q; Millipore). Cetuximab was kindly provided by ImClone Systems Inc. Female severe combined immunodeficiency (SCID) mice were purchased from Charles River. A cell disrupter (Sonifier; Branson), tissue homogenizer (Tekmar), and centrifuge (RC2-B; Sorvall) were used in receptor-binding experiments. Size-exclusion high-performance liquid chromatography (HPLC) used in conjugation and purification of radiolabeled conjugate was accomplished on an HR 10/300 column (Superose 12; Amersham Biosciences) with a 2487 dual λ absorbance detector (Waters) and a radioactive detector (Ortec, model 661; EG&G Instruments). The mobile phase consisted of 20 mM 4-(2-hydroxyethyl)-1-piperazineethanesulfonic acid and 150 mM sodium chloride, pH 7.3, eluted at a flow rate of 0.5 mL/min. Millennium 32 software (Waters) was used to quantify chromatograms by integration. An 8000 automated well-type γ -counter (Beckman) was used to measure the activity of size-exclusion HPLC fractions of animal biodistribution samples and for internalization samples. Levels of radioactivity higher than 0.037 MBq (1 μCi) during radiosynthesis were assayed in a dose calibrator (model-15R; Capintec; Ramsey, NJ). MultiScreen 96-well microtiter plates (Millipore) for receptor-binding assays were measured on a 1450 Microbeta Trilux Liquid Scintillation and Luminescence Counter (PerkinElmer Life Sciences). ^{64}Cu was produced on a biomedical cyclotron CS-15 at Washington University School of Medicine, as previously reported (11).

Cell Culture

CaSki and HeLa cell lines were purchased from American Type Culture Collection, and DoTc2 4510, C-33A, and ME-180 cell lines were provided by F. Patrick Ross, Washington University School of Medicine. Cell culture medium was purchased from Gibco, fetal

bovine serum (FBS) from Hyclone, and all other medium supplements from the Washington University School of Medicine Tissue Culture Support Center. C-33A and HeLa cells were maintained in Eagle's minimum essential medium (EMEM) in Earle's balanced salt solution and 2 mM L-glutamine modified to contain 1.5 g of sodium bicarbonate per liter, supplemented with 1 mM nonessential amino acids, 10 mM sodium pyruvate, and 10% FBS. CaSki cells were maintained in RPMI 1640 medium with 2 mM L-glutamine modified to contain 10 mM 4-(2-hydroxyethyl)-1-piperazineethanesulfonic acid, 1 mM sodium pyruvate, 4.5 g of glucose per liter, and 1.5 g of sodium bicarbonate per liter, supplemented with 10% FBS. DoTc2 4510 cells were maintained in Dulbecco's modified Eagle's medium with 4 mM L-glutamine modified to contain 4.5 g of glucose per liter and 1.5 g of sodium bicarbonate per liter, supplemented with 10% FBS. ME-180 cells were maintained in McCoy's 5a medium with 1.5 mM L-glutamine and 2.2 g of sodium bicarbonate per liter, supplemented with 10% FBS.

EGFR Gene Expression

In the context of a parallel study designed to perform molecular profiling on cervical cancer cell lines, 2 mcg of cellular RNA were analyzed on U133Plus2 gene expression microarrays (Affymetrix) using standard protocols provided by the manufacturer. Biotinylated target preparation, array hybridization, and scanning were performed by the Siteman Cancer Center Multiplexed Gene Analysis Core facility. From the microarray dataset of 23 cell line samples, probe set data for the EGFR transcript (4 independent probe sets) were extracted, normalized across all arrays in the experiment, and used to compare relative transcript abundance of EGFR.

Preparation of ^{64}Cu -DOTA-Cetuximab

DOTA was conjugated to cetuximab in 0.1 M disodium phosphate (Na_2HPO_4) (pH 7.5) using an adaptation of the method described by Lewis et al. (12). Cetuximab (2 mg/mL) was washed with 0.1 M Na_2HPO_4 (pH 7.5) using a YM-100 centrifugal filter device (Centricon) and then concentrated. DOTA-mono-NHS ester was dissolved in 0.1 M Na_2HPO_4 (pH 7.4), and pH was adjusted to 7.4 by adding 0.1 M sodium hydroxide. An aliquot of this solution was added to the concentrated cetuximab in a 120:1 molar ratio of DOTA-mono-NHS ester to cetuximab and followed by incubation at 4°C overnight with end-over-end rotation. The conjugate was then transferred to a Centricon YM-100, diluted to 2.0 mL with 0.1 M ammonium citrate (pH 5.5), and centrifuged. This procedure was repeated to remove small-molecule reactants, and the conjugate was collected from the membrane. Purity and concentration of the resulting DOTA-cetuximab conjugate were determined by size-exclusion HPLC. Titration of DOTA-cetuximab with ^{64}Cu -copper acetate spiked with ^{64}Cu using a previously published method (13) revealed that the ratio of DOTA to cetuximab achieved by this procedure was 5:5.

Radiolabeling of DOTA-cetuximab with ^{64}Cu was performed by adding approximately 100 μg of the conjugate to 19–74 MBq (0.5–2 mCi) of $^{64}\text{CuCl}_2$ in 0.1 M ammonium citrate buffer, pH 5.5, followed by a 1-h incubation at 40°C. The radiochemical purity of the resulting ^{64}Cu -DOTA-cetuximab was determined by size-exclusion HPLC and radio-thin-layer chromatography. If necessary, ^{64}Cu -DOTA-cetuximab was challenged with 10 mM ethylenediamine tetraacetic acid (5 μL) to complex-free ^{64}Cu . ^{64}Cu -DOTA-cetuximab was then isolated with a desalt spin column (0.5 mL) (Zeba; Pierce) to obtain radiochemical purities greater than 95%. Specific activity of the final product was 0.93 GBq/mg (25 mCi/mg).

A previous study reported the synthesis of ^{64}Cu -DOTA-cetuximab with a specific activity of 1.24 GBq/mg, with 21.5 DOTA residues per cetuximab (14).

Receptor Binding of ^{64}Cu -DOTA-Cetuximab

Assays were performed with live cells using a modification of a previously described method (15). ^{64}Cu -DOTA-cetuximab (0.05–10 nM) was incubated with cell monolayers of the 5 cervical cancer cell lines in 24-well plates for 2 h at 4°C in their respective growth media. CaSki, ME-180, and DoTc2 4510 cells contained 1×10^5 cells/well (525 cells/mm²); HeLa cells contained 5×10^4 cells/well (260 cells/mm²); and C-33A cells contained 1.5×10^5 cells/well (790 cells/mm²). The cells were washed twice with 1 mL of ice-cold Hanks' balanced salt solution and lysed by incubation at 90°C in 0.9 mL of 0.1 M sodium hydroxide for 30 min. Aliquots of each sample were analyzed for protein by a bicinchoninic acid assay. Samples were transferred into microfuge tubes and counted in a γ -counter. Nonspecific binding was determined in parallel assays containing an excess (200 nM) of unlabeled cetuximab. Specific binding was obtained by subtracting nonspecific binding from total binding and was corrected for total protein content. Dissociation constants in nM and maximum receptor densities (B_{max}) in fmol/mg were estimated by nonlinear fitting of the specific binding versus the concentration of ^{64}Cu -DOTA-cetuximab using Prism software (GraphPad).

Internalization of ^{64}Cu -DOTA-Cetuximab

Cells (approximately 5×10^5 /well) were seeded in 6-well plates containing their respective growth medium and were incubated at 37°C in 5% CO₂, until 80% confluent. On the day of the assay, the medium was aspirated and replaced with 3 mL of fresh growth medium. For determination of unspecific internalization of ^{64}Cu -DOTA-cetuximab, 1 set of wells was incubated with unlabeled cetuximab (1,000-fold excess) at 37°C in 5% CO₂ for 10 min to block receptors. ^{64}Cu -DOTA-cetuximab (133.2 kBq [3.6 μCi], 0.38 μg /15 μL) was added and incubated at 37°C in 5% CO₂ for various time points, after which the radioactive medium was aspirated and the plate was washed twice with 2 mL of phosphate-buffered saline (PBS). To collect the surface-bound fraction of this receptor-mediated process, each well was treated with 20 mM sodium acetate in PBS (pH 3.0) and was incubated at 4°C for 10 min and then followed by a second wash with 20 mM sodium acetate in PBS (pH 3.0) without incubation, which was pooled with the first rinse. The cellular fraction was dissolved with 0.5% sodium dodecyl sulfate in PBS. All of the fractions were counted for radioactivity with a γ -counter. The percentage internalized was the amount of activity in the final cell pellet, corrected for activity in the blocked fractions and background activity and normalized to protein content.

Tumor Xenografts

CaSki tumors were grown in female SCID mice by following a modification of the protocol of Cairns and Hill (16). Cells (5×10^6) were implanted subcutaneously in the flank, and palpable tumors were observed 3–4 wk after implantation.

In Vivo Biodistribution and Small-Animal PET Imaging

Animal studies were conducted in accordance with the highest standards of care as outlined in the National Institutes of Health *Guide for Care and Use of Laboratory Animals* (17) and the policy and procedures for animal research at Washington University School of Medicine. After injection of aliquots of ^{64}Cu -DOTA-cetuximab (100 μL , 555 kBq [15 μCi]) via the tail vein, blood,

organs, and tumors were removed from animals sacrificed at 24 h after injection ($n = 5$). Radioactivity of tissue samples was measured with a γ -counter. The percentage injected activity per gram (%ID/g) was calculated by comparison with standards representing the injected dose per animal.

For imaging studies, mice bearing CaSki tumors were anesthetized by inhalation of 2% isoflurane, injected with ^{64}Cu -DOTA-cetuximab (7,400 kBq [200 μCi], 20 μg), and scanned at 24 h after injection on a small-animal PET device (Focus, model 120 or 220; Concorde Microsystems Inc.). High-resolution coregistration micro-CT imaging was performed to monitor tumor volume and morphology at 24 h after injection. All small-animal PET images were reconstructed, and regional tracer concentrations were quantified by use of the ASIPRO software package (Concorde Microsystems Inc.). Quantitative data were expressed as standardized uptake values, which are defined as the counts per second per pixel in a region of interest encompassing the entire organ divided by total counts per second per pixel in the mouse.

RESULTS

Twenty-three human cervical cancer cell lines (including several identical cell lines grown in different laboratories) were analyzed by gene expression microarray analysis. Among the approximately 54,000 probe sets represented on the array, 4 probe sets representing the EGFR transcript were analyzed to characterize EGFR transcript levels in each line (Fig. 1). Cell lines were classified according to their level of EGFR expression from the averaged probe set signals. In addition, cDNA templates from each of the cell lines were used to perform double-stranded resequencing of the entire EGFR coding region. None of the cell lines demonstrated previously characterized sequence alterations either within or external to the EGFR coding domain (data not shown).

Five cervical cancer cell lines, covering the entire range of EGFR mRNA expression, were selected for further study: CaSki (high EGFR expression), ME-180 and DoTc2 4510 (both midrange EGFR expression), HeLa (low EGFR expression), and C-33A (negative for EGFR expression).

To determine the relationship between EGFR gene expression levels and cell-surface expression of the EGFR, saturation receptor binding of ^{64}Cu -DOTA-cetuximab to the EGFR was performed. Binding studies were performed in live cells at 4°C to inhibit internalization and trafficking of cetuximab. The results are shown in Figure 2.

In Figure 2, 4 of the 5 cell lines exhibited saturable ^{64}Cu -DOTA-cetuximab binding. The fifth line, C-33A, showed no specific ^{64}Cu -DOTA-cetuximab binding. The affinity of ^{64}Cu -DOTA-cetuximab binding for the EGFR was similar in the 4 EGFR-positive lines, varying from 0.1 to 0.7 nM. These values are consistent with those reported for the binding of unmodified cetuximab to the EGFR (dissociation constant, 0.1–0.4 nM) (18). Therefore, conjugation to DOTA and complexation with ^{64}Cu did not affect the affinity of cetuximab toward its antigen. The B_{max} for ^{64}Cu -DOTA-cetuximab binding to these cell lines paralleled the levels of EGFR expression determined by microarray analysis (Fig. 2; Table 1).

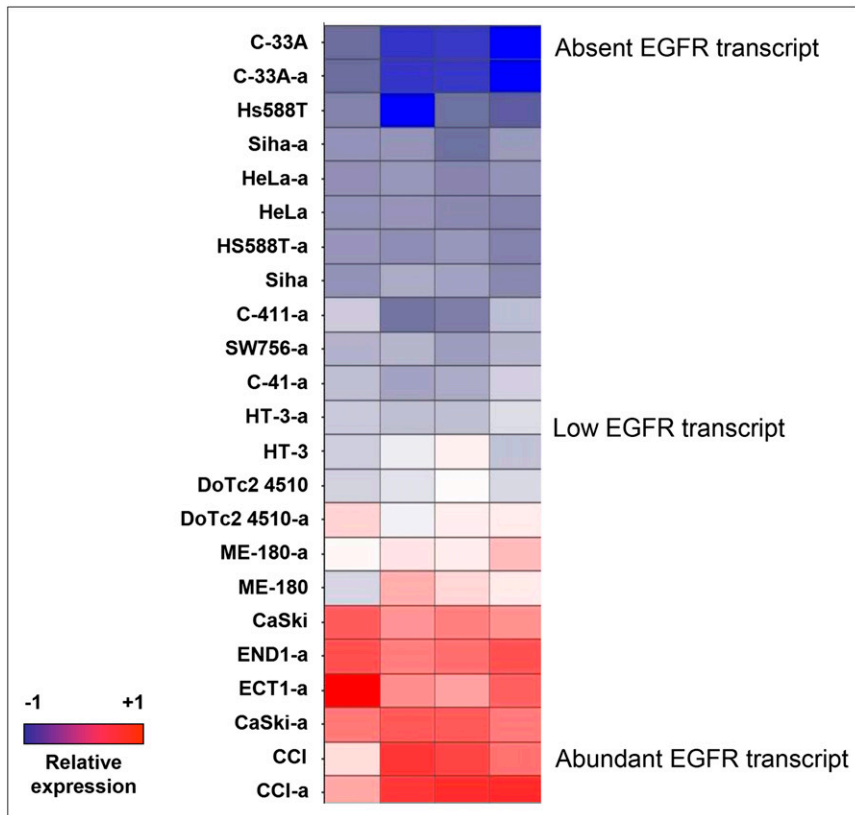


FIGURE 1. Transcriptional profiling of cervical cancer cell lines with U133Plus2 GeneChip microarrays (Affymetrix). EGFR expression is based on 4 different oligonucleotide probe sets (each column shows response to 1 probe set). Cell lines are ordered based on their relative levels of EGFR probe signals. Cell lines with suffix designation “-a” were grown and harvested independently.

Internalization assays were next performed to determine whether EGFR number correlated with increased uptake of ^{64}Cu -DOTA-cetuximab by receptor-mediated endocytosis. For these experiments, cells were incubated with ^{64}Cu -DOTA-cetuximab at 37°C , and internalization was measured

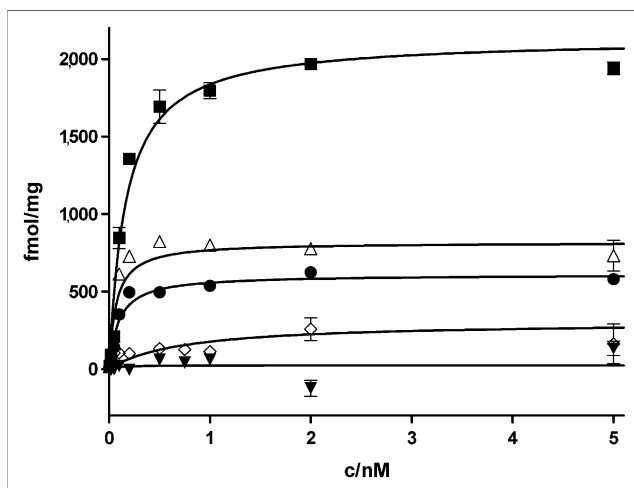


FIGURE 2. Saturation receptor binding of ^{64}Cu -DOTA-cetuximab to 5 cervical cancer cell lines ($n = 3$). EGFR densities (B_{max} in fmol/mg) on cell surface were, from high to low, CaSki (\blacksquare , $2,130 \pm 60$) > ME-180 (\triangle , 820 ± 40) > DoTc2 4510 (\bullet , 610 ± 20) > HeLa (\diamond , 310 ± 110) > C-33A (\blacktriangledown , not applicable).

by determining the amount of cell-associated ^{64}Cu -DOTA-cetuximab that was stable to acid wash (PBS) supplemented with 20 mM sodium acetate, pH 3.0. The data in Figure 3A show that all EGFR-positive cell lines internalized ^{64}Cu -DOTA-cetuximab. Internalization was linear for the first 15–30 min but began to plateau after approximately 1 h. No uptake was observed in the EGFR-negative C-33A cells. The maximum level of internalization observed after 4 h paralleled receptor expression levels as determined by ^{64}Cu -DOTA-cetuximab saturation binding (Table 1).

To determine whether the difference in uptake was because of an increase in the rate of internalization, ^{64}Cu -DOTA-cetuximab uptake was followed over a 15-min time course, and the data were plotted as the ratio of internalized ^{64}Cu -DOTA-cetuximab to cell-surface ^{64}Cu -DOTA-cetuximab versus time. This normalizes uptake to receptor number and allows assessment of the rate of internalization on a per-receptor basis. Figure 3B shows that the slopes of the InSur plots were similar for all 4 EGFR-positive cell lines, indicating that the rate of uptake was similar in all lines. Thus, the difference in the absolute amount of ^{64}Cu -DOTA-cetuximab internalized can be attributed to differences in the number of cell-surface EGFRs.

In CaSki cells, the line that expressed the highest level of EGFRs, approximately 50,000 fmol of ^{64}Cu -DOTA-cetuximab per milligram were internalized within 4 h. This corresponds to an internalized ^{64}Cu -DOTA-cetuximab-to-

TABLE 1
Quantification of EGFR mRNA and Protein Levels in 5 Cervical Cancer Cell Lines

Cell line	EGFR expression	B _{max} (fmol/mg)	Internalization at 4 h (fmol/mg)	Ligand molecules internalized-to-receptor ratio
CaSki	++++	2,130 ± 60	50,500 ± 1,000	24
ME-180	+++	820 ± 40	22,700 ± 400	28
DoTc2 4510	++	610 ± 20	15,500 ± 400	25
HeLa	+	310 ± 110	6,100 ± 100	20
C-33A	-	NA	NA	NA

NA = not applicable.

receptor ratio of 24 (Table 1). This correspondence suggests that the EGFRs are continuously recycled to the cell surface rather than being targeted into the degradation pathway. The ratio of internalized ⁶⁴Cu-DOTA-cetuximab to EGFR number was similar for the ME-180 (28), DoTc2 4510 (25), and HeLa (20) cells, indicating that all lines exhibited the same phenomenon of receptor recycling followed by cetuximab-induced receptor internalization.

To assess the interaction of ⁶⁴Cu-DOTA-cetuximab with cervical cancer cells *in vivo*, 5 × 10⁶ CaSki cells were injected into female SCID mice. Three weeks later, palpable tumors were observed. ⁶⁴Cu-DOTA-cetuximab was then injected into these tumor-bearing athymic nude mice (n = 5), and its biodistribution was assessed 24 h after injection (Fig. 4). Uptake into the cervical cancer cell tumor was high (13.2 ± 1.2 %ID/g). By contrast, uptake was low in muscle (3.4 ± 0.2 %ID/g) and bone (2.6 ± 0.2 %ID/g). However, uptake in other nontarget organs remained high at 24 h, especially in the blood (23.8 ± 0.9 %ID/g) and the spleen (25.6 ± 1.7 %ID/g). This biodistribution at 24 h indicates that optimal contrast is likely observed at time points greater than 24 h after injection, which is consistent with data from Cai et al. (14) and data from our group (15).

A preliminary small-animal PETCT experiment was performed in a CaSki tumor-bearing mouse that showed high ⁶⁴Cu-DOTA-cetuximab uptake in the tumor mass but

relatively low nontarget uptake 24 h after injection (Fig. 5). The specific uptake value for the tumor was 1.39, whereas the values for the liver and heart were 1.72 and 1.63, respectively. These data are consistent with the biodistribution data, indicating relatively high liver and blood accumulation, although the tumor is visible at 24 h.

DISCUSSION

Despite widespread screening for cervical cancer, this disease continues to claim lives, particularly among medically underserved populations of women. Gardasil (Merck & Co., Inc.), a recombinant vaccine against human papilloma virus types 6, 11, 16, and 18, was approved by the Food and Drug Administration in 2006 and by the European Union in 2007. Although this is an important step in the battle against cervical cancer, the viral types for which this vaccine provides protection are responsible for only 70% of the cases of cervical cancer. Also, the vaccine will provide no protection for women who have already been exposed to the target strains (19). Therefore, the need for advances in the diagnosis and treatment of cervical cancer will persist.

Cetuximab has been approved in Europe and the United States for the clinical treatment of advanced metastatic colorectal cancer and advanced head and neck cancer. Like cervical cancer, these tumors are known to express elevated

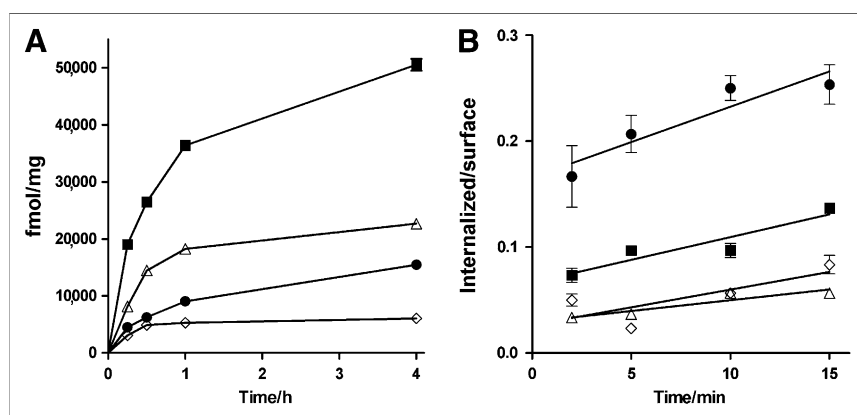


FIGURE 3. Internalization of ⁶⁴Cu-DOTA-cetuximab (n = 3). (A) Internalization standardized to protein mass over 4 h displayed same relative order as seen by expression profiling and receptor binding: CaSki (■) > ME-180 (Δ) > DoTc2 4510 (●) > HeLa (◇). (B) Rate of internalization in first 15 min of exposure to ⁶⁴Cu-DOTA-cetuximab, displayed as internalized to surface-bound activity.

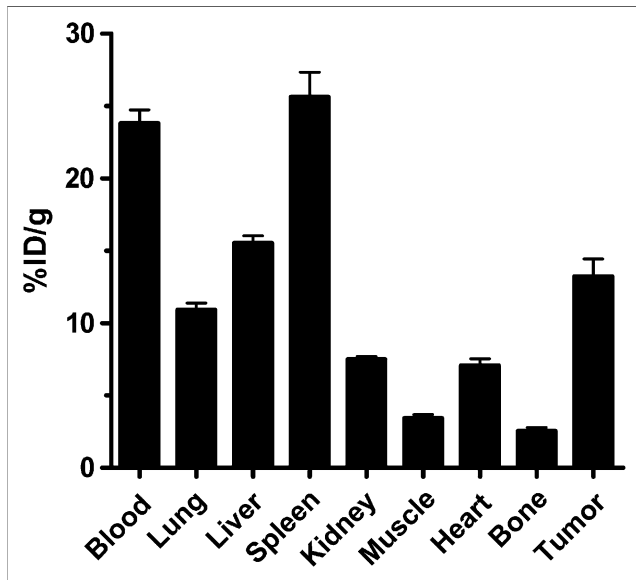


FIGURE 4. Biodistribution of ^{64}Cu -DOTA-cetuximab in CaSki tumors implanted into SCID mice at 24 h after injection.

levels of EGFRs (20,21). The studies presented here were aimed at investigating the use of cetuximab in the diagnosis and subtyping of cervical cancers.

Microarray analysis of 23 human cervical cancer cell lines demonstrated significant differences among lines in the level of expression of EGFR mRNA. Thus, the sensitivity of these tumors to cetuximab-induced cell killing is likely to be highly variable. In particular, tumors that do not express EGFRs are not likely to be effectively targeted by cetuximab.

To determine the potential use of cetuximab in identifying EGFR-positive cell lines, we conjugated cetuximab with DOTA and radiolabeled it with ^{64}Cu . This radionuclide (half life, 12.7 h; β^+ , 17.4%; β^- , 41%) emits both β^+ and β^- radiation, allowing for the use of ^{64}Cu radiopharmaceuticals with high tumor-to-background ratios for both PET imaging and targeted radiotherapy of cancer.

We used ^{64}Cu -DOTA-cetuximab to quantify EGFR levels and found that the expression of EGFR mRNA correlated with the number of cell-surface EGFR in 5 human cervical cancer cell lines. In addition, the degree of ^{64}Cu -DOTA-cetuximab internalization correlated with both EGFR mRNA and protein levels. CaSki cells, which showed the highest EGFR mRNA levels by microarray analysis, were also found to have the highest maximum density of EGFR per milligram of protein. In addition, they internalized more ^{64}Cu -DOTA-cetuximab than did the other cell lines. At the other end of the spectrum, C-33A cells responded negatively to all oligonucleotide probe sets, and no EGFR could be detected by ^{64}Cu -DOTA-cetuximab-binding assays. Thus, ^{64}Cu -DOTA-cetuximab binding appears to be a useful probe for quantifying EGFR number and function.

Several recent reports have investigated whether the response of colorectal tumors to cetuximab therapy is correlated with EGFR mRNA copy number or EGFR protein levels. Moroni et al. (21) demonstrated a correlation between response to cetuximab and increased EGFR gene copy number in patients with metastatic colorectal cancer. By contrast, Vallböhmer et al. (22) failed to find a significant correlation between colorectal tumor EGFR mRNA levels and patient response to cetuximab, but this study was hampered by a small sample size. Nonetheless, it was observed that patients with higher levels of gene expression of the

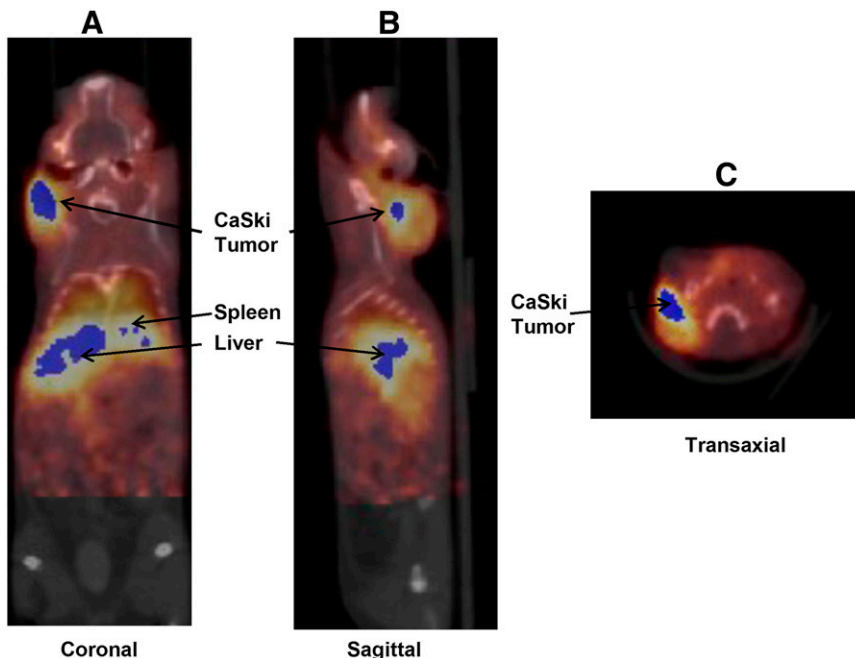


FIGURE 5. Small-animal PET imaging of ^{64}Cu -DOTA-cetuximab in CaSki tumor-bearing SCID mice at 24 h after injection: coronal (A), sagittal (B), and transaxial (C) views.

EGFR had a shorter overall survival. Despite these correlations, 1 study of patients with colorectal cancer with no detectable tumor levels of EGFR as determined by immunohistochemistry showed that approximately 25% of these patients respond to cetuximab (23). The data presented in these studies suggest that the quantification of EGFR by immunohistochemistry is unreliable and demonstrate the need for a more sensitive method for measuring EGFR for use in stratifying patients for potential response to cetuximab. Molecular imaging of EGFR with PET/CT and cetuximab labeled with a positron emitter, compared with traditional methods, may be a sensitive alternative measure of EGFR.

To assess the potential for ^{64}Cu -DOTA-cetuximab as a PET/CT agent, a preliminary study was performed in which ^{64}Cu -DOTA-cetuximab was injected into nude mice bearing tumors derived from CaSki cervical cancer cells. Biodistribution analysis demonstrated high uptake of ^{64}Cu -DOTA-cetuximab in implanted CaSki tumors at 24 h after injection ($13.2 \pm 1.2\%$ ID/g). This result is comparable to the highest level of uptake of ^{64}Cu -DOTA-cetuximab in a recent study of 7 tumor cell lines implanted in athymic nude mice (14). The uptake in the liver was comparable in both studies ($14.0 \pm 1.4\%$ ID/g at 16 h after injection vs. $15.5 \pm 0.5\%$ ID/g at 24 h after injection in our study), but retention of radiopharmaceutical in the blood was significantly higher in our system (14). Copper can dissociate from the chelator DOTA, which may in part account for the observed uptake in nontarget organs. The use of bifunctional chelators that form more stable copper complexes, such as 4,11-bis(carboxymethyl)-1,4,8,11-tetraazabicyclo[6.6.2]hexadecane (CB-TE2A), can alleviate copper dissociation and reduce nonspecific copper uptake (24). However, CB-TE2A is labeled with ^{64}Cu at 95°C and a pH greater than 8 (25). Antibodies are denatured under these conditions, and until suitable prelabeling procedures for ^{64}Cu -CB-TE2A with subsequent conjugation to antibodies are available, it will be necessary to use chelators that can be radiolabeled under milder conditions. At any rate, that uptake of ^{64}Cu -DOTA-cetuximab into CaSki tumors was readily detected in our studies and that its extent of uptake correlates with EGFR number suggests that further examination of this radiopharmaceutical with additional time points with the CaSki model, as well as imaging of EGFRs in other cervical cancer mouse models, is warranted.

CONCLUSION

We demonstrated that the expression of EGFR mRNA correlated well with protein levels of EGFR as determined by ^{64}Cu -DOTA-cetuximab. In addition, the levels of internalization of ^{64}Cu -DOTA-cetuximab in the 5 cervical cancer cell lines corresponded to the EGFR density, and the rates of internalization were similar. As several studies have demonstrated that EGFR densities in tumors do not typically correlate with response to cetuximab therapy, questions arise as to whether determination of EGFR concentration in tumors with ^{64}Cu -DOTA-cetuximab and PET would be a

more valuable tool than immunohistochemistry and less invasive than tumor biopsy followed by mRNA analysis. Data presented here strongly suggest that ^{64}Cu -DOTA-cetuximab is an accurate biomarker of EGFR expression levels, and this agent with PET might be useful for patient selection and therapeutic monitoring with all types of EGFR inhibitors, including small-molecule and antibody-based, although further imaging studies are warranted.

ACKNOWLEDGMENTS

We thank Susan Adams and Christopher Sherman for technical assistance, Jerrel Rutlin for small-animal PET/CT image analysis, and Wenping Li for helpful discussions. Cetuximab was provided by ImClone Systems. This research was supported by National Cancer Institute (NCI) grant P50CA9405604. The production of ^{64}Cu at Washington University School of Medicine was supported by NCI grant R24 CA86307. Small-animal imaging at Washington University School of Medicine was supported by NIH grant 5 R24 CA83060.

REFERENCES

1. Jemal A, Tiwari RC, Murray T, et al. Cancer statistics, 2004. *CA Cancer J Clin*. 2004;54:8–29.
2. Hougardy BM, Maduro JH, van der Zee AG, Willemse PH, de Jong S, de Vries EG. Clinical potential of inhibitors of survival pathways and activators of apoptotic pathways in treatment of cervical cancer: changing the apoptotic balance. *Lancet Oncol*. 2005;6:589–598.
3. Laskin JJ, Sandler AB. Epidermal growth factor receptor: a promising target in solid tumours. *Cancer Treat Rev*. 2004;30:1–17.
4. Salomon DS, Brandt R, Ciardiello F, Normanno N. Epidermal growth factor-related peptides and their receptors in human malignancies. *Crit Rev Oncol Hematol*. 1995;19:183–232.
5. Kim JW, Kim YT, Kim DK, Song CH, Lee JW. Expression of epidermal growth factor receptor in carcinoma of the cervix. *Gynecol Oncol*. 1996;60:283–287.
6. Scambia G, Ferrandina G, Distefano M, D'Agostino G, Benedetti-Panici P, Mancuso S. Epidermal growth factor receptor (EGFR) is not related to the prognosis of cervical cancer. *Cancer Lett*. 1998;123:135–139.
7. Kimmig R, Pfeiffer D, Landsmann H, Hepp H. Quantitative determination of the epidermal growth factor receptor in cervical cancer and normal cervical epithelium by 2-color flow cytometry: evidence for down-regulation in cervical cancer. *Int J Cancer*. 1997;74:365–373.
8. Kersemaekers AM, Fleuren GJ, Kenter GG, et al. Oncogene alterations in carcinomas of the uterine cervix: overexpression of the epidermal growth factor receptor is associated with poor prognosis. *Clin Cancer Res*. 1999;5:577–586.
9. Kim YT, Park SW, Kim JW. Correlation between expression of EGFR and the prognosis of patients with cervical carcinoma. *Gynecol Oncol*. 2002;87:84–89.
10. Kim GE, Kim YB, Cho NH, et al. Synchronous coexpression of epidermal growth factor receptor and cyclooxygenase-2 in carcinomas of the uterine cervix: a potential predictor of poor survival. *Clin Cancer Res*. 2004;10:1366–1374.
11. McCarthy DW, Shefer RE, Klinkowstein RE, et al. Efficient production of high specific activity ^{64}Cu using a biomedical cyclotron. *Nuclear Med Biol*. 1997;24:35–43.
12. Lewis MR, Boswell CA, Laforest R, et al. Conjugation of monoclonal antibodies with TETA using activated esters: biological comparison of ^{64}Cu -TETA-1A3 with ^{64}Cu -BAT-2IT-1A3. *Cancer Biother Radiopharm*. 2001;16:483–494.
13. Sun X, Rossin R, Turner JL, et al. An assessment of the effects of shell cross-linked nanoparticle size, core composition, and surface PEGylation on in vivo biodistribution. *Biomacromolecules*. 2005;6:2541–2554.
14. Cai W, Chen K, He L, Cao Q, Koong A, Chen X. Quantitative PET of EGFR expression in xenograft-bearing mice using ^{64}Cu -labeled cetuximab, a chimeric anti-EGFR monoclonal antibody. *Eur J Nucl Med Mol Imaging*. 2007;34:850–858.
15. Li WP, Meyer LA, Capretto DA, Sherman CD, Anderson CJ. Receptor binding, biodistribution, and metabolism studies of ^{64}Cu -DOTA-cetuximab, a PET

- imaging agent for epidermal growth-factor receptor-positive tumors. *Cancer Biother Radiopharm.* 2008;23:158–171.
16. Cairns RA, Hill RP. A fluorescent orthotopic model of metastatic cervical carcinoma. *Clin Exp Metastasis.* 2004;21:275–282.
 17. *Guide for the Care and Use of Laboratory Animals.* Washington, DC: National Academy Press; 1996.
 18. Goldstein NI, Prewett M, Zuklys K, Rockwell P, Mendelsohn J. Biological efficacy of a chimeric antibody to the epidermal growth factor receptor in a human tumor xenograft model. *Clin Cancer Res.* 1995;1:1311–1318.
 19. Hanna E, Bachmann G. HPV vaccination with Gardasil: a breakthrough in women's health. *Expert Opin Biol Ther.* 2006;6:1223–1227.
 20. Wong SF. Cetuximab: an epidermal growth factor receptor monoclonal antibody for the treatment of colorectal cancer. *Clin Ther.* 2005;27:684–694.
 21. Moroni M, Veronese S, Benvenuti S, et al. Gene copy number for epidermal growth factor receptor (EGFR) and clinical response to antiEGFR treatment in colorectal cancer: a cohort study. *Lancet Oncol.* 2005;6:279–286.
 22. Vallböhmer D, Zhang W, Gordon M, et al. Molecular determinants of cetuximab efficacy. *J Clin Oncol.* 2005;23:3536–3544.
 23. Chung KY, Shia J, Kemeny NE, et al. Cetuximab shows activity in colorectal cancer patients with tumors that do not express the epidermal growth factor receptor by immunohistochemistry. *J Clin Oncol.* 2005;23:1803–1810.
 24. Wadas TJ, Wong EH, Weisman GR, Anderson CJ. Copper chelation chemistry and its role in copper radiopharmaceuticals. *Curr Pharm Des.* 2007;13:3–16.
 25. Wadas TJ, Anderson CJ. Radiolabeling of TETA- and CB-TE2A-conjugated peptides with copper-64. *Nat Protoc.* 2006;1:3062–3068.